

Observed and simulated estimates of the meridional overturning circulation at 26.5° N in the Atlantic

J. Baehr^{1,*}, S. Cunningham², H. Haak³, P. Heimbach¹, T. Kanzow^{2,**}, and J. Marotzke³

¹Massachusetts Institute of Technology, Cambridge, MA, USA

²National Oceanography Centre, Southampton, UK

³Max Planck Institute for Meteorology, Hamburg, Germany

* now at: Institute of Oceanography, KlimaCampus, University of Hamburg, Grindelberg 5, 20144 Hamburg, Germany

** now at: IFM-GEOMAR, Kiel, Germany

Received: 2 June 2009 – Published in Ocean Sci. Discuss.: 1 July 2009

Revised: 13 October 2009 – Accepted: 30 October 2009 – Published: 16 November 2009

Abstract. Daily timeseries of the meridional overturning circulation (MOC) estimated from the UK/US RAPID/MOCHA array at 26.5° N in the Atlantic are used to evaluate the MOC as simulated in two global circulation models: (I) an 8-member ensemble of the coupled climate model ECHAM5/MPI-OM, and (II) the ECCO-GODAE state estimate. In ECHAM5/MPI-OM, we find that the observed and simulated MOC have a similar variability and time-mean within the 99% confidence interval. In ECCO-GODAE, we find that the observed and simulated MOC show a significant correlation within the 99% confidence interval. To investigate the contribution of the different transport components, the MOC is decomposed into Florida Current, Ekman and mid-ocean transports. In both models, the mid-ocean transport is closely approximated by the residual of the MOC minus Florida Current and Ekman transports. As the models conserve volume by definition, future comparisons of the RAPID/MOCHA mid-ocean transport should be done against the residual transport in the models. The similarity in the variance and the correlation between the RAPID/MOCHA, and respectively ECHAM5/MPI-OM and ECCO-GODAE MOC estimates at 26.5° N is encouraging in the context of estimating (natural) variability in climate simulations and its use in climate change signal-to-noise detection analyses. Enhanced confidence in simulated hydrographic and transport variability will require longer observational time series.

1 Introduction

The evaluation of basin-wide mass and heat transports in the ocean components of climate models is difficult since such transports have until recently not been monitored. The basin-wide mass transport is typically considered in the form of the meridional overturning circulation (MOC), the zonally and vertically integrated meridional transport as a function of latitude and depth. MOC timeseries represent the northward transport at a certain latitude. Here, we use the term “MOC” for a timeseries of the maximum northward transport, i.e. the northward transport integrated to a depth where this transport reaches a maximum. While such a timeseries is readily computed in a numerical model, direct observations of the MOC would require basin-wide full-depth coverage of the meridional velocities. In March 2004, the RAPID/MOCHA mooring array was deployed in the North Atlantic with the purpose of providing a continuous estimate of the zonally integrated meridional mass transport at 26.5° N (Cunningham et al., 2007; Kanzow et al., 2007). Here, we use the first year of the RAPID/MOCHA MOC estimates to evaluate the MOC variability in two ocean climate models.

The RAPID/MOCHA array is based on a conceptual study by Marotzke et al. (1999), suggesting that the MOC can be continuously monitored using measurements of the density at the eastern and western boundaries of a zonal section. The RAPID/MOCHA array consists of profiles of density and ocean bottom pressure along 26.5° N, with dense coverage at the western and eastern boundaries as well as on both sides of the Mid Atlantic Ridge (Marotzke et al., 2002; Rayner, 2005). Prior to deployment, Hirschi et al. (2003) and Baehr et al. (2004) tested the array in two numerical models, showing that such an array should be capable of capturing both the



Correspondence to: J. Baehr
(johanna.baehr@zmaw.de)

time-mean of the MOC as well as the daily to annual variability. The simulated array was also capable of detecting long-term trends within several decades as shown by Baehr et al. (2008) with a (univariate) MOC timeseries from a climate simulation forced with the Intergovernmental Panel on Climate Change (IPCC) scenario A1B (Nakicenovic and Swart, 2000).

Prior to RAPID/MOCHA, most observation-based MOC estimates have relied on occasional hydrographic transects (e.g. Hall and Bryden, 1982; Roemmich and Wunsch, 1985; Bryden et al., 2005; Longworth and Bryden, 2007). As pointed out by various authors (e.g. Wunsch and Heimbach, 2006; Baehr et al., 2008), a time series of such transects represents sparse sampling (once every few years or decades) with serious aliasing problems, complicating estimates of variability or trends. Dynamically consistent ocean state estimates from the ECCO project have recently become available covering either the timespan of the altimetric record after 1992 (Wunsch and Heimbach, 2006), or going back to the beginning of the NCEP/NCAR reanalysis period in 1952 (Köhl and Stammer, 2008). These ocean state estimates attempt to bring a general circulation model (the MITgcm; Marshall et al., 1997) to consistency with most of the observations available from the global observing system. To the extent that statistical consistency can be achieved within prior uncertainty estimates, any oceanic quantity, including meridional heat and mass transports, can be derived from the full three-dimensional ocean state, providing an alternative observation-based estimate of that quantity.

Here, we use the RAPID/MOCHA array MOC estimate from the first deployment period (March 2004–March 2005) to evaluate the MOC as simulated in two numerical models. We evaluate two different numerical models: (I) the coupled global climate model ECHAM5/MPI-OM (e.g. Jungclaus et al., 2006), whose simulations were performed as part of a suite of experiments for the IPCC Fourth Assessment Report, (II) the global oceanic state estimate ECCO-GODAE (Wunsch and Heimbach, 2007), a model constrained by least squares to a multitude of data-sets. For ECCO-GODAE, we use results of a solution that was optimised from 1992 to 2004. To cover the full observational period, a forward run was continued beyond the period of optimisation, i.e. using the forcing directly from the re-analysis products. Originally, the continuation of the forward run with unadjusted surface forcing was an act of necessity. However, in ultimately aiming to predict the MOC, we see this as a primitive test of ECCO-GODAE's capability to resemble the observations by using an optimised initial state. Note that the RAPID/MOCHA observations were not used as constraints for these runs.

The dissimilitude of the two numerical models results in different expectations for the evaluation against the RAPID/MOCHA MOC estimate. While we expect ECCO-GODAE to reproduce the RAPID/MOCHA MOC estimate in both its temporal and spatial structure, we expect

ECHAM5/MPI-OM to provide an ensemble of possible projections whose basic statistics are comparable to the observed MOC, though without close resemblance to the short-term temporal structure. The main objective of the present study is therefore to evaluate the modelled MOC against the RAPID/MOCHA MOC timeseries as a reference estimate. In an accessory note, we test how to compute the MOC and its contributions analogously in both the observations and the numerical models.

Throughout the paper, we refer to the RAPID/MOCHA MOC estimate as the “observed” MOC, and the model-based estimates as the “simulated” MOC. This should, however, not imply that the RAPID/MOCHA MOC estimate can be taken as a direct observation of the MOC, as it is based on inferring transports from hydrographic measurements. Also, the contribution of eddies to the total transport variability is still a matter of discussion (Wunsch, 2007; Kanzow et al., 2009). Note that the horizontal resolution of both models (1.5° in ECHAM5/MPI-OM, and 1° in ECCO-GODAE) is too coarse to resolve eddies.

Here, we focus on the RAPID/MOCHA MOC estimate at 26.5° N in the Atlantic, or more specifically, on the zonal density gradient and the resulting meridional transports. This focus should not imply that other observations of the hydrography at 26.5° N and elsewhere such as XBTs, altimeter, ARGO floats, and their incorporation into global ocean observing systems, do not provide an essential piece in assessing the North Atlantic circulation. However, the unique coverage of the 26.5° N line warrants a detailed analysis of the variability of meridional transports and their relation to the boundary densities at 26.5° N. After introducing the details of the dataset and the two models (Sect. 2), we therefore start with a comparison of the boundary densities (Sect. 3). We then analyse the meridional transports both in depth classes and through a dynamical decomposition (also in Sect. 3). A discussion follows in Sect. 4, conclusions in Sect. 5.

2 Data and models

2.1 The RAPID/MOCHA array

The RAPID/MOCHA array has been designed to provide a continuous estimate of the strength and vertical structure of the MOC across 26.5° N continuously. The resulting MOC estimate is the sum of three observable components constrained to hold mass balance: the mid-ocean transport, the Florida Current transport, and the Ekman transport. Below, we describe how each of these components is obtained.

The mid-ocean transport is the sum of the mid-ocean geostrophic transport and the meridional transport west of the westernmost density mooring (“western boundary wedge transport”). The mid-ocean geostrophic transport between the Bahamas and the coast of West Africa is derived from the difference between vertical density profiles from the eastern

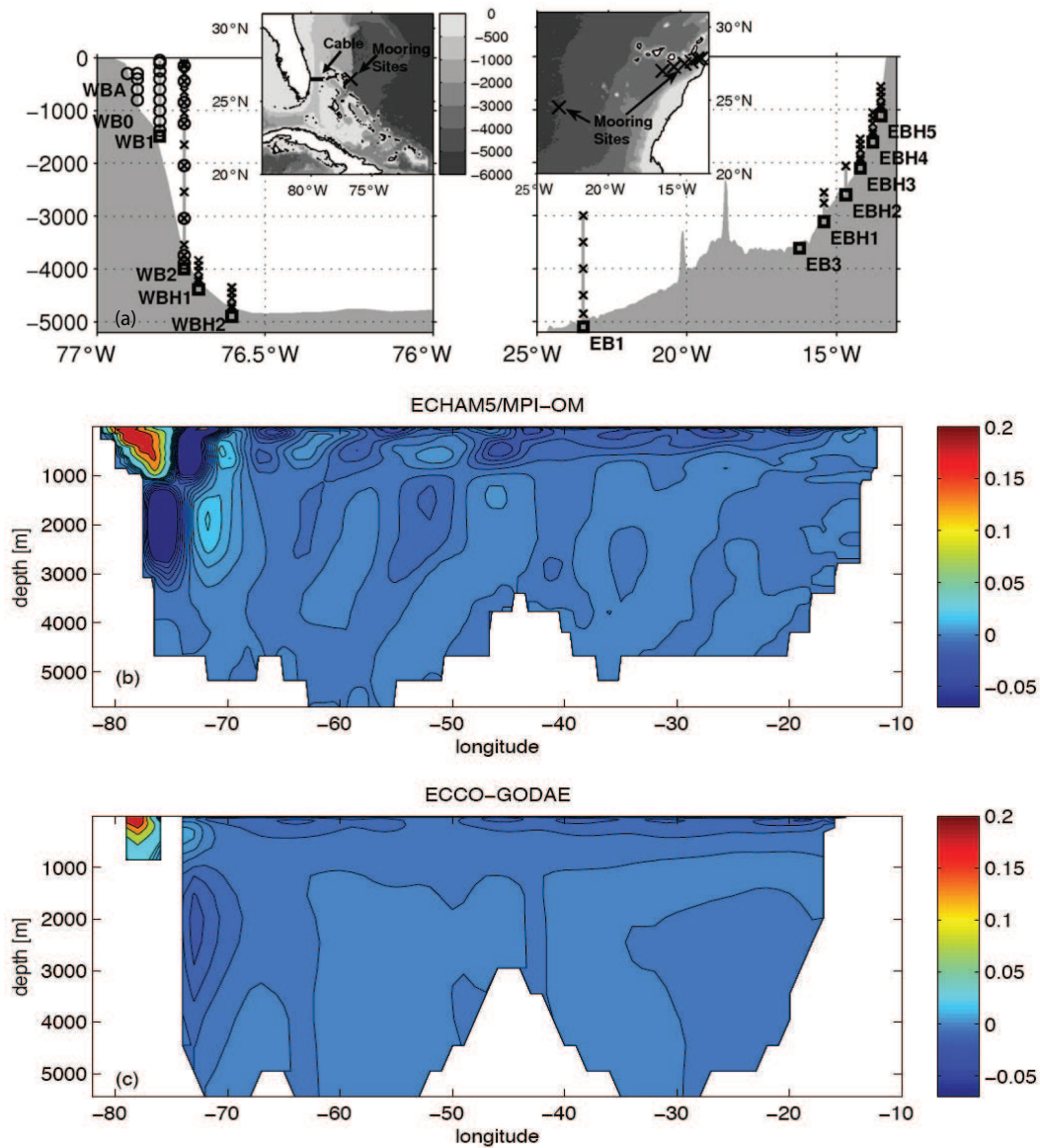


Fig. 1. Zonal transect at 26.5° N. (a) RAPID/MOCHA array moorings near the western (left) and eastern (right) boundary. The dynamic height profiles were composed at the western boundary from WB2, WBH2, and WBH1, and at the eastern boundary from EB1, EBH1, ..., EBH5 (for details see Cunningham et al., 2007 and Kanzow et al., 2007). Moorings WBA, WB0, WB1, and WB2 provided velocity measurements, used to derive the western boundary wedge transport (for details see Johns et al., 2007). Note the different zonal scales. (b) Time mean meridional velocity for March 2004–March 2005 in ECHAM5/MPI-OM. (c) Time mean meridional velocity for March 2004–March 2005 in ECCO-GODAE. Contour lines are only shown between -0.05 and 0.05 cm s^{-1} .

and western boundaries at 26.5° N of the Atlantic (Fig. 1, top panel). As in Cunningham et al. (2007) and Kanzow et al. (2007), we use merged profiles at both boundaries. For the western boundary profile, temperature and salinity measurements from the moorings WB2, WBH1 and WBH2 have been merged; for the eastern boundary profile, the moorings EB1, EBH1, EBH2, EBH3, EBH4 and EBH5 have been merged. From these density profiles, the geostrophic mid-ocean transport, relative to 4820 dbar is computed. Note that

the MOC estimate of Cunningham et al. (2007) does not include the profiles at the Mid Atlantic Ridge. The western boundary wedge transport is the meridional transport west of the westernmost density mooring WB2 (Fig. 1, top left panel), where the upper ocean Antilles current and a small fraction of the deep western boundary current reside, is estimated by direct current meter measurements from 19 sensors on 4 moorings covering the range between the sea surface and 2000 dbar (Johns et al., 2007).

The magnitude of northward flow of the Gulf Stream through the Straits of Florida (“Florida Current”) is observed by measuring the flow-induced voltage in a telephone cable, which runs along the sea floor between Florida and the Bahamas (Larsen, 1985; see also small inset in Fig. 1, top left panel). This observing system is maintained by the US National Oceanic and Atmospheric Administration and has provided daily estimates of Gulf Stream transport for over 20 years now (Baringer and Larsen, 2001).

The zonally integrated Ekman transport between the Bahamas and the coast of West Africa is computed from the zonal component of the wind stress, which is inferred from space-borne scatterometry (Graf et al., 1998) on a daily basis.

In order to derive daily estimates of the MOC profile between 29 March 2004 and 31 March 2005, Cunningham et al. (2007) then imposed the net mid-ocean geostrophic transport to balance the sum of Gulf Stream, Ekman transport plus western boundary wedge transport. They achieved this balance by adding to the relative mid-ocean geostrophic transport profile a barotropic transport flow such that mass was conserved at each time step. Kanzow et al. (2007) did not constrain the flow but referenced the time-variable part of the relative mid-ocean geostrophic transport (but not the time mean) using differences in bottom pressure measurements taken at the base of each of the density moorings (Fig. 1). They found the various transport contributions to be in mass balance at periods longer than 10 days, thus providing evidence for the validity of the MOC monitoring strategy and, specifically, justifying the mass balance constraint used by Cunningham et al. (2007), for timescales longer than 10 days. Here, we analyse the daily transport timeseries as this allows a direct evaluation of the simulated MOC against the published timeseries of Cunningham et al. (2007).

2.2 ECHAM5/MPI-OM

The coupled ECHAM5/MPI-OM global climate model consists of the atmospheric component ECHAM5 (Roeckner et al., 2003), which is coupled to the ocean component MPI-OM (Marsland et al., 2003); no flux adjustments are applied. ECHAM5 is realised at T63 spectral resolution ($\approx 140 \times 210$ km grid spacing at mid-latitudes) with 31 vertical levels. MPI-OM is realised on an orthogonal curvilinear C-grid (Marsland et al., 2003). To avoid the singularity at the geographical North Pole, the northern grid pole is shifted to Greenland. MPI-OM has an average horizontal resolution of about 1.5° , varying between 12 km close to Greenland and 180 km in the tropical Pacific. In the vertical, there are 40 non-equidistant z -levels, of which 20 are distributed over the top 700 m. The bottom topography is resolved by partial grid cells. Jungclauss et al. (2006) described the coupled model’s ocean mean state, based on an unperturbed control simulation and forced with present-day greenhouse gas concentrations. For the computation of the volume transport, velocities from the curvilinear ECHAM5/MPI-OM grid

are transformed back to a regular latitude-longitude grid (with 0.25 degree resolution), before calculating transports at 26.5° N. The back transformation results in an additional time-mean mass imbalance of approximately 0.5 Sv.

Here, we analyse eight realisations forced by three different climate change greenhouse gas scenarios, performed for the IPCC Assessment Report 4. Initially, three realisations start from different years of the control run, in which pre-industrial greenhouse gas concentrations are applied. These three realisations are forced with observed greenhouse gas and aerosol concentrations for the years 1860 to 2000. For the years 2001 to 2005, the simulations are forced with greenhouse gas concentrations based on the IPCC emission scenarios B1 (three realisations), A1B (three realisations), and A2 (two realisations) (Nakicenovic and Swart, 2000). As the impact of the difference between scenarios with respect to MOC trends is small during the short time interval considered here, we can consider the simulations as realisations of the same experiment. Thus the analysed ensemble consists of eight realisations with daily output from March 2004 to March 2005.

Note that due to its horizontal resolution ECHAM5/MPI-OM does not resolve the Bahamas, and therefore the western boundary current is not geographically confined (Fig. 1). Here, we compute the Florida Current transport over a fixed spatial area: we integrate from the western boundary to the first gridpoint outside the northward boundary current, and from the surface to a depth where transports are close to zero (here, over about 800 km in the zonal direction, and about 1000 m in the vertical). Note that this definition of the area for the Florida Current includes the whole northward western boundary current in the model, that is, nominally both the Gulf Stream and the Antilles Current. Additionally, the definition includes a time varying recirculation component, which is in the time-mean a southward transport of about 4 Sv. However, computing the transport over a fixed spatial area (in contrast to a certain dynamical criterion) allows us to separate the contributions by the “Florida Current” from those by the “interior”, as if the transport were geographically confined to the Straits of Florida. Zonal and meridional windstress in ECHAM5/MPI-OM are calculated using the actual velocity differences between ocean and atmosphere at the surface.

2.3 ECCO-GODAE

The second simulation used in the present study is the quasi-global ocean state estimate produced by the ECCO-GODAE (Estimating the Circulation and Climate of the Ocean – Global Ocean Data Assimilation Experiment) project. This product succeeds the first generation ECCO estimates published by Stammer et al. (2002, 2003). ECCO-GODAE attempts to bring the MIT general circulation model (MITgcm) (Marshall et al., 1997) to consistency with as many observations as practical globally within estimated uncertainties.

The reduction of the quadratic model versus data misfit (the so-called cost function) is achieved via a gradient descent method. The gradient of the cost function with respect to initial conditions and time-varying air-sea fluxes is computed via the adjoint of the MITgcm (Marotzke et al., 1999; Heimbach et al., 2005), the code of which has been derived by means of the automatic differentiation (AD) tool TAF (Giering and Kaminski, 1998). An overview of the method is provided by Wunsch and Heimbach (2007) (see also <http://www.ecco-group.org> for an overall account of efforts within the ECCO Consortium).

The ECCO-GODAE setup covers the world ocean between 80° N and 80° S, excluding the Arctic, at 1° horizontal resolution and using 23 vertical levels. An earlier version, termed version 1, of the 1° solution was produced at Scripps Institution of Oceanography and covered 1992 through 2001 (Köhl et al., 2007). For version 2 of the production, taken on at MIT and Atmospheric and Environmental Research (AER), the estimation period has been extended through 2004 (and soon will be extended through 2007). The number of iterations in the optimisation have been augmented from 69 (version 1) to 216 (version 2). ECCO-GODAE incorporates a multitude of datasets, e.g., hydrographic observations such as CTD sections, XBTs, sea surface temperature, but also scatterometer, altimeter, and a mean dynamic topography (for a complete list see Table A1 of Wunsch and Heimbach, 2006). Many additional observations have been added for version 2, notably temperature and salinity profiles from the Argo floats available since 2004. The World Ocean Atlas (1994), which served as initial condition and climatological constraint, has been replaced below 300 m depth by the WOCE atlas of Gouretski and Koltermann (2004). Note that in order to produce a full estimate overlapping the RAPID record through mid 2005 the ECCO-GODAE solution has been integrated forward in time beyond the estimation period, i.e. without fitting to observations for 2005. After 2004, we use unadjusted fields for the surface forcing. Thus the ECCO-GODAE solution provided here is a prediction of the oceanic state after December 2004, assuming the atmospheric state is known after December 2004.

Despite its limited horizontal resolution, ECCO-GODAE resolves the Bahamas, but the Straits of Florida span over nearly 400 km (Fig. 1), compared with about 100 km width in the real ocean. To the east of the Bahamas ECCO-GODAE's ocean interior is bounded by a wall, preventing the western boundary continental slope from being resolved (Fig. 1). Most of the northward transport goes through the Straits of Florida; the Antilles Current has a time mean between 1 and 2 Sv (not shown), which is smaller than the 6 Sv observed by Meinen et al. (2004). The standard deviation of the Antilles Current is about 2.5 Sv for ECCO-GODAE compared with 3 Sv observed by Meinen et al. (2004).

3 Results

3.1 Hydrographic characteristics and east-west density gradient

We analyse the hydrographic characteristics of both the eastern and the western boundaries, which set the thermal wind balance for the interior flow above the crest of the Mid Atlantic Ridge. For the RAPID/MOCHA array, we use the merged profiles of Cunningham et al. (2007); Kanzow et al. (2007) as described in Sect. 2.1. Similarly, merged profiles are used for the models: for the western boundary, a single profile at the location of the WB2 mooring is used (as the locations of the other moorings are not resolved); for the eastern boundary, vertical profiles eastward of the location of EB1 have been merged. The RAPID/MOCHA array observations show that for the time-mean over the observational period of one year, the thermocline (above 800 m) at the western boundary is up to 4°C warmer and up to 0.5 more saline than the eastern boundary (Fig. 2). In the intermediate water (800–1100 m), the western boundary is cooler by up to 3°C and fresher by up to 0.2 than the eastern boundary, a characteristic diminishing with depth, but found for the entire upper North Atlantic Deep Water (upper NADW; 1100–3000 m). For the lower NADW (below 3000 m), the western boundary is warmer by about 0.1°C than the eastern boundary, whereas salinities are similar.

In ECHAM5/MPI-OM, both the temperature and the salinity are considerably higher than the RAPID/MOCHA array observations at both boundaries. At the western boundary the ECHAM5/MPI-OM ensemble average is 4°C warmer and nearly 0.4 saltier than the observations at 1000 m depth (Fig. 2). The discrepancies persist at 2000 m depth with about half of the 1000 m magnitudes. The eastern boundary shows similar discrepancies as the western boundary for temperature, while the discrepancies between observations and model are larger than at the western boundary for salinity (up to 0.7), and most pronounced above 1500 m (Fig. 2).

The discrepancies in the temperature and salinity fields result in generally lighter water in ECHAM5/MPI-OM than in the observations (not shown). At the western boundary, the discrepancy between the model density and the observations is largest at 1000 m (0.5 kg m^{-3}), but considerably smaller below. At the eastern boundary, the discrepancy in the density field at 1000 m is about 0.3 kg m^{-3} , as it is at 2000 m. Below 1500 m, the east-west density difference in ECHAM5/MPI-OM shows little similarity to the one observed with respect to both magnitude and sign (Fig. 3). Between about 500 m and 1000 m, ECHAM5/MPI-OM's density difference is stronger than observed, while between about 2000 m and 3000 m it is weaker than observed.

In ECCO-GODAE, the discrepancies to the RAPID/MOCHA array observations are smaller overall than in ECHAM5/MPI-OM (Fig. 2). The RAPID/MOCHA array observations and the ECCO-GODAE solution overlap

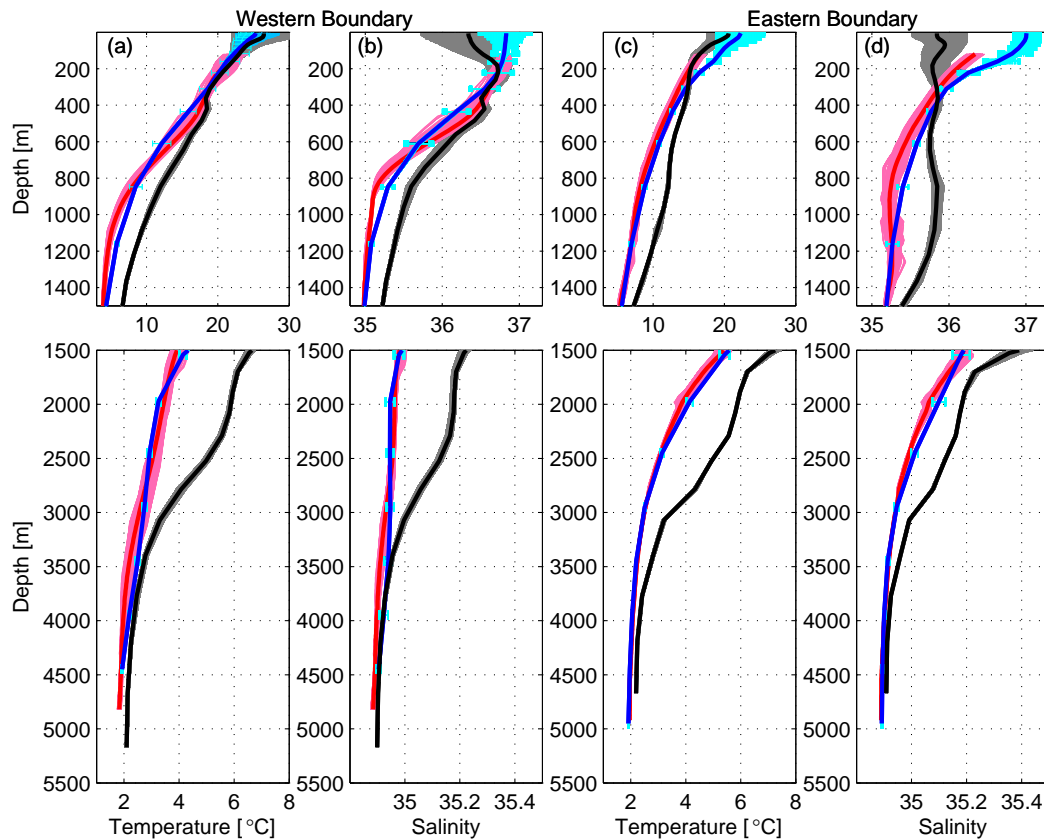


Fig. 2. Merged potential temperature and salinity profiles for RAPID/MOCHA array observations (pink, time-mean: red), ECHAM5/MPI-OM (ensemble members: grey, time-mean of ensemble mean: black) and ECCO-GODAE (light blue, with uncertainties based on Forget and Wunsch (2007), time-mean: blue): (a) potential temperature at the western boundary, (b) salinity at the western boundary, (c) potential temperature at the eastern boundary, (d) salinity at the eastern boundary. For the RAPID/MOCHA array, the shallowest data are at 120 m depth.

at all depths below 200 m within the estimated uncertainties of Forget and Wunsch (2007). Several discrepancies are noteworthy. At the western boundary, ECCO-GODAE is about 1°C colder than the observations at around 500 m, and about 1°C warmer than the observations at around 1000 m (Fig. 2). The salinities at the eastern boundary show a similar discrepancy as at the western boundary: 0.2 fresher at around 500 m, and 0.1 more saline at around 1000 m. At the eastern boundary, ECCO-GODAE is about 0.5°C warmer than the observations between about 500 m and 1000 m. Further, the eastern boundary in ECCO-GODAE is persistently more saline than the observations (up to 0.15). Note that the local salinity maximum in the observations at the eastern boundary at about 1200 m is not reproduced by ECCO-GODAE (Fig. 2). At the eastern boundary the top 1000 m are generally more saline in ECCO-GODAE than in the observations, and therefore the salinities at 1200 m match by coincidence.

As a consequence of the discrepancies in temperature and salinity at the western boundary, densities are higher by up to 0.2 kg m^{-3} in ECCO-GODAE than in the observations, in the depth range of 500 m to 1000 m. Between 1100 m and 2000 m, ECCO-GODAE is lighter than the observations by up to 0.1 kg m^{-3} (not shown). At the eastern boundary, ECCO-GODAE is lighter than the observations by up to 0.03 kg m^{-3} above 500 m, and between 1100 and 2000 m. In the basin-wide east-west density gradient, some of the discrepancies cancel each other. Overall, the zonal density gradient in ECCO-GODAE is similar to the RAPID/MOCHA array observations, that is, exhibiting the same sign across nearly all depths (Fig. 3), while weaker in ECCO-GODAE than observed above 1500 m, and generally stronger below. Discrepancies are largest at the surface and between about 1000 and 1100 m. At this depth, the zonal density gradient is slightly negative in the observations, but slightly positive in ECCO-GODAE due to comparatively warm water at the western boundary.

Table 1. Layer transports, excluding the Florida Current and Ekman transport: time-mean and standard deviations (std), both in [Sv].

	RAPID/MOCHA		ECHAM5/MPI-OM		ECCO-GODAE	
	mean	std	mean	std	mean	std
Thermocline (above 800 m)	-16.4	2.7	-36.5	3.3	-18.0	1.8
Intermediate (800–1100 m)	0.6	0.6	-3.3	0.6	-1.8	0.8
upper NADW (1100–3000 m)	-11.0	3.1	-21.1	2.7	-11.9	2.2
lower NADW (below 3000 m)	-8.0	3.5	1.3	3.5	0.7	3.0

3.2 Meridional layer transports

The discrepancies in the east-west density gradients are directly mirrored in the vertical structure of the mid-ocean transport (Fig. 4; cf. Fig. 1 of Cunningham et al., 2007).

As described in Sect. 2, the mid-ocean transport for the RAPID/MOCHA array is the sum of the western boundary wedge transport and the mid-ocean geostrophic transport calculated from the density profiles at the boundaries. The modeled mid-ocean transport is based on utilizing the full meridional velocity fields as provided by the models.

Overall, the time-means of ECHAM5/MPI-OM’s transports are mostly outside the observed range, while the time-means of ECCO-GODAE’s transports are mostly inside the observed range, with the exception of intermediate depths and transports below about 4000 m. The latter discrepancy results to a large extent from differences in the computation of the mid-ocean transports. While the observational estimate is based on thermal wind and essentially ignoring the Mid Atlantic Ridge (Kanzow et al., 2007), the model transports are computed from the full meridional velocity field. Computing the mid-ocean transports in the numerical models similarly to the observations, i.e. from east-west density gradients, results in a structure similar to the observations with small southward transport at depth instead of northward transport (not shown). Note that the estimates based on the five hydrographic occupations of the transect show southward transports between 3000 and 5000 m, and small northward transports at about 5500 m (Bryden et al., 2005, their Fig. 2).

To quantify the discrepancies in the mid-ocean transport, we compute the transports in layers (Fig. 5, Table 1; cf. Fig. 2 of Cunningham et al., 2007). Two discrepancies from the RAPID/MOCHA transport estimates are common to both models: (I) at intermediate depths, none of the models shows northward transport, but instead small southward transports of about 2 Sv, and (II) below 3000 m, both models show weak northward transports of about 1 Sv, whereas the RAPID/MOCHA transport estimates show a strong southward transport of 8 Sv. In ECHAM5/MPI-OM, thermocline and upper NADW transports have strengths of about 20 Sv and 10 Sv, respectively, in the time-mean, considerably higher than the RAPID/MOCHA transport estimates. In

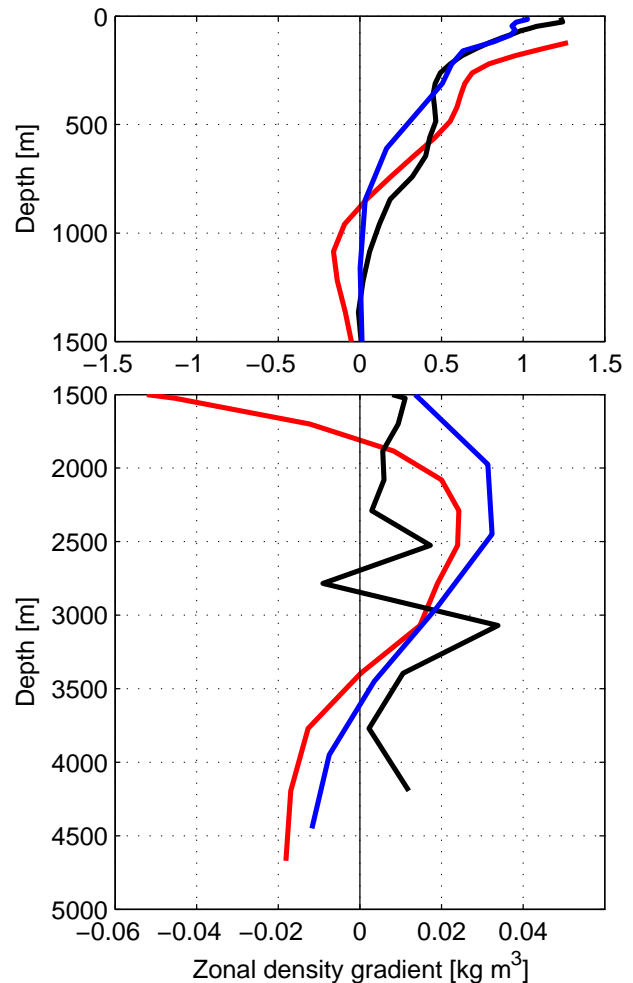


Fig. 3. Observed and modelled zonal density difference (eastern boundary minus western boundary; time-mean). Red: RAPID/MOCHA. Black: ECHAM5/MPI-OM. Blue: ECCO-GODAE.

contrast, the corresponding ECCO-GODAE estimates are of comparable magnitudes to the RAPID/MOCHA estimates, within 2 Sv in the time-mean.

The large variability of the transports at different depths is reproduced by the models to some extent (Fig. 5, Table 1):

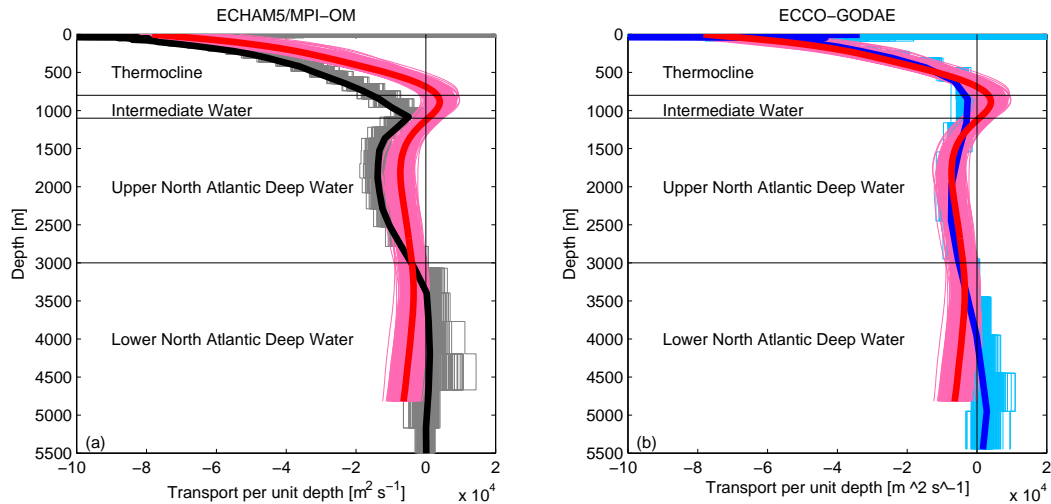


Fig. 4. Vertical profiles of mid-ocean transport per unit depth [$\text{m}^2 \text{s}^{-2}$], excluding Florida Current and Ekman transport from RAPID-MOC array (red; as in Cunningham et al. (2007), Fig. 1) and models: (a) ECHAM5/MPI-OM (black; one realisation), (b) ECCO-GODAE (blue). Bold lines indicate the time-mean, light shading the variability over the observation period.

in the thermocline, RAPID/MOCHA shows a standard deviation of 2.7 Sv, while ECHAM5/MPI-OM has a slightly higher standard deviation of 3.3 Sv, and ECCO-GODAE has a slightly lower standard deviation of 1.8 Sv. The intermediate transport variability is similar among all three estimates (standard deviation of 0.6 Sv for RAPID/MOCHA, 0.6 Sv for ECHAM5/MPI-OM, 0.8 Sv for ECCO-GODAE). Note that the time-means of the simulated intermediate transports are of opposite sign to the observed transport. The variability of the upper NADW is 3.1 Sv in the RAPID/MOCHA observations, and 2.7 Sv in ECHAM5/MPI-OM, while ECCO-GODAE underestimates the variability (2.2 Sv). The lower NADW shows similar variability in all estimates (3.5 Sv for RAPID/MOCHA, 3.5 Sv for ECHAM5/MPI-OM, 3.0 Sv for ECCO-GODAE), while the time-mean in both models is more than 5 Sv smaller than from the RAPID/MOCHA array.

3.3 Mid-ocean transport

Integrating the mid-ocean transport vertically results in the basin-wide geostrophic transport contribution to the MOC. In the observations, the MOC is then derived by adding the Ekman and Florida Current transport to the mid-ocean transport. While earlier model studies suggested that this sum is a close proxy for the MOC (Hirschi et al., 2003; Baehr et al., 2004), it is not a direct measurement of the MOC. In the numerical models, we therefore test two different computations of the models' mid-ocean transport: the mid-ocean transport is computed (I) dynamically similar to the RAPID/MOCHA mid-ocean transport estimate, (II) kinematically similar to the RAPID/MOCHA mid-ocean transport estimate.

- (I) Dynamically, the RAPID/MOCHA mid-ocean transport estimate (based on Cunningham et al., 2007) is the western boundary wedge transport plus the mid-ocean geostrophic transport (east-west density difference, referenced to 4820 dbar) integrated from the surface to the depth at which the sign of the transport switches from northward to southward. In the models, the limited horizontal resolution does not allow us to distinguish between western boundary wedge transport and mid-ocean geostrophic transport when computing the mid-ocean transport. Note further that the mid-ocean transport is southward at all depths in both models, and we therefore integrate to a depth at which the velocities are close to zero (about 1000 m).
- (II) Kinematically, the RAPID/MOCHA mid-ocean transport estimate is part of the transports yielding the full MOC, which is the sum of the mid-ocean transport, the Florida Current transport, and the Ekman transport (Cunningham et al., 2007). In the numerical models, the MOC is readily computed as the full meridional velocity field is available. Therefore, by reversing the decomposition employed by RAPID/MOCHA, the mid-ocean transport can also be computed by subtracting the Florida Current transport and the Ekman transport from the MOC.

The differences between the two methods mostly indicate to what extent the mid-ocean transport can be estimated by the east-west density gradient (similar to what has been analysed by e.g. Hirschi et al. (2003); Baehr et al. (2004)). Therefore, the limitations of the dynamical method are those of a thermal wind calculation (level of no motion, bottom

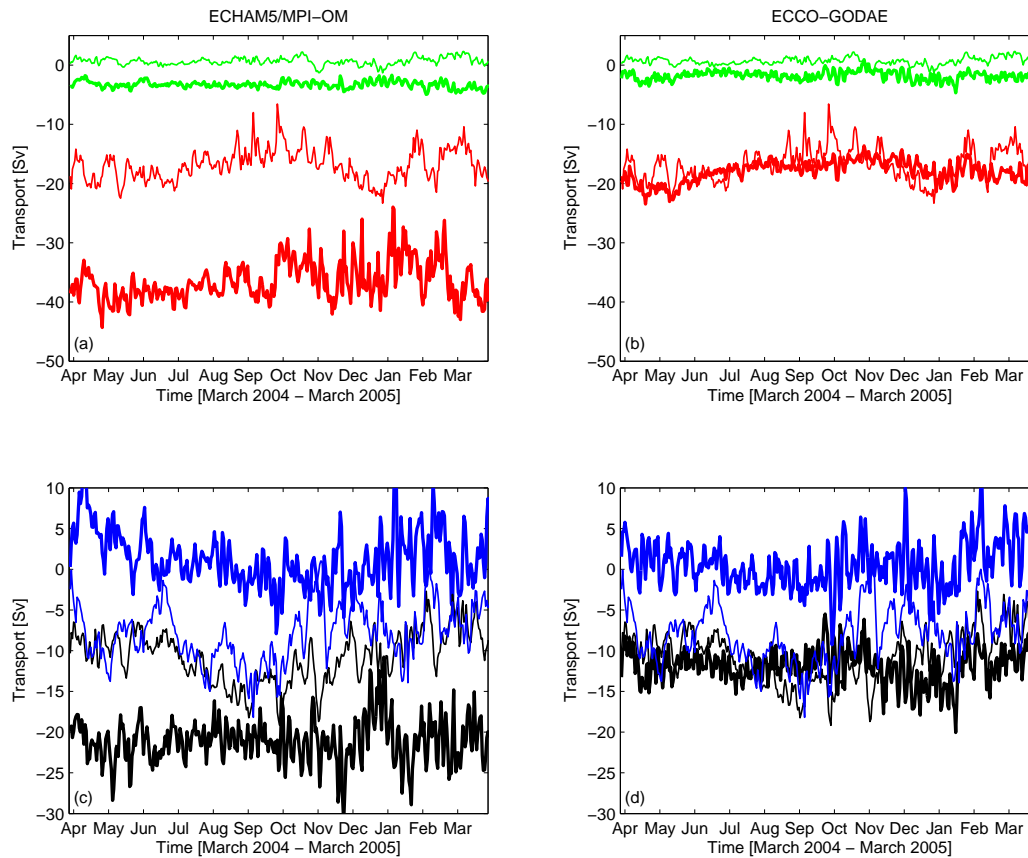


Fig. 5. Integrated layer transports excluding Florida Current and Ekman transport from RAPID-MOC array (thin; as in Cunningham et al. (2007), Fig. 2) and models (thick): **(a)** and **(b)** thermocline (above 800 m, red), intermediate (800–1100 m, green); **(c)** and **(d)** upper North Atlantic Deep Water (NADW, 1100–3000 m, black), lower NADW (below 3000 m, blue). (a) and (c) ECHAM5/MPI-OM (one realisation). (b) and (d) ECCO-GODAE.

triangles, ...). Here, however, the focus is less on testing thermal wind, but identifying the appropriate method to compare modelled and observed MOC estimates.

In ECHAM5/MPI-OM, definition (I) results in a timeseries with higher variability than definition (II): 4.8 Sv compared with 3.8 Sv standard deviation (Fig. 6, and Table 3), and also in a stronger time-mean by more than 10 Sv. This difference in the time-mean in ECHAM5/MPI-OM is sensitive to the chosen level of no motion, which was taken to be consistent with RAPID/MOCHA, but is not necessarily an adequate choice in the model. In contrast, in ECCO-GODAE definition (I) results in a timeseries with lower variability than does definition (II) with a standard deviation of 1.4 Sv compared with 2.1 Sv; the time-mean is similar for both definitions. Placing the level of no motion in ECCO-GODAE at the bottom shows similar time-mean and variability as in definition (II), suggesting that the differences between the definitions emerging in ECHAM5/MPI-OM are specific to the model.

We therefore utilise the kinematic definition (II) of the mid-ocean transport for the subsequent analysis in both models, assuming that it represents the mid-ocean transport as in the RAPID/MOCHA array observations. In other words, we rely on the model's ability to represent the large scale meridional flow field in a dynamically consistent way, whereas we attribute the differences in the simulated observations (mostly ECHAM5/MPI-OM) to model limitations. On a rather technical note, the above results therefore suggest employment of the kinematic definition (II) for future evaluations of the simulated MOC against observations.

3.4 MOC decomposition

To compute the MOC at 26.5° N, we use the decomposition used to compute the RAPID/MOCHA MOC estimate (Cunningham et al., 2007): $MOC = \text{Florida Current transport} + \text{Ekman transport} + \text{mid-ocean transport}$. For the numerical models, we compute the MOC as the zonally and vertically integrated transport above about 1000 m. The Ekman

Table 2. Time mean and standard deviations (std) of different meridional transport components, both in [Sv]. Last row shows the mean of standard deviations for the ensemble members (as opposed to the standard deviation of the ensemble mean). Shading indicates where the mean/standard deviation (variance) are within the 99 percent confidence intervals of the RAPID/MOCHA array estimates. Black box indicates significant correlation within the 95 percent confidence interval.

	MOC		FC		Ekman		basin	
	mean	std	mean	std	mean	std	mean	std
RAPID/MOCHA array	19.1	5.6	31.7	3.3	3.0	4.4	-15.6	3.1
ECCO-GODAE	11.4	4.2	26.5	2.8	3.7	3.8	-18.8	2.1
ECHAM5/MPI-OM A1B	18.9	4.8	43.2	3.8	5.4	4.2	-29.7	3.8
ECHAM5/MPI-OM A1B	18.7	5.8	43.4	4.0	5.3	4.3	-30.0	4.2
ECHAM5/MPI-OM A1B	19.1	4.4	40.8	3.7	6.3	4.2	-28.0	4.6
ECHAM5/MPI-OM B1	18.7	4.4	43.4	3.2	6.3	3.9	-31.1	3.5
ECHAM5/MPI-OM B1	19.7	5.0	43.2	3.4	7.5	4.2	-31.1	3.4
ECHAM5/MPI-OM B1	19.3	5.2	42.8	3.4	6.1	4.2	-29.7	4.3
ECHAM5/MPI-OM A2	17.6	5.6	41.2	3.9	4.3	4.9	-28.3	3.8
ECHAM5/MPI-OM A2	17.5	5.4	40.5	3.8	4.9	4.3	-27.9	3.6
mean of ECHAM5/MPI-OM ensemble	18.7	5.1	42.4	3.7	5.8	4.3	-29.5	3.9

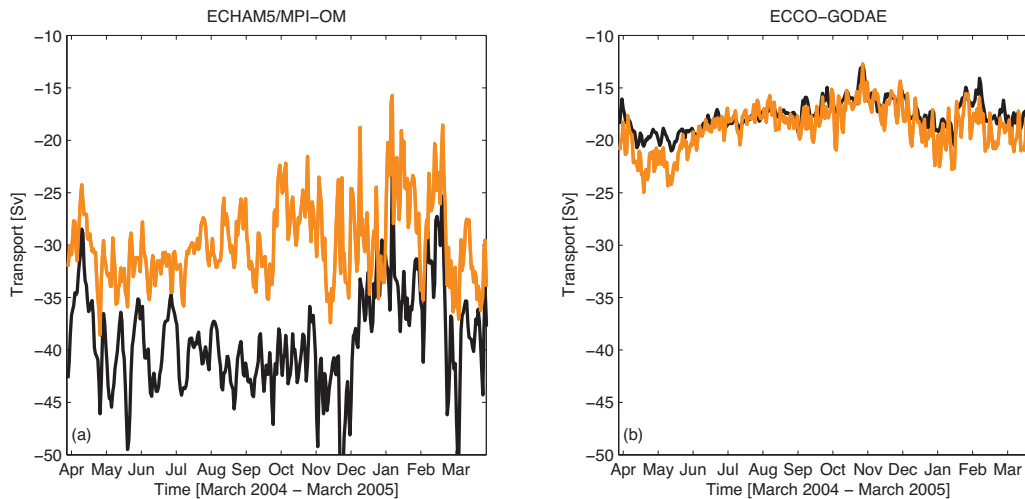


Fig. 6. Modelled transports. Different computations of the mid-ocean transport: (I) the mid-ocean transport computed equivalently to the RAPID/MOCHA estimate (Cunningham et al., 2007) (black). (II) residual = MOC – Florida – Current – Ekman (orange). (a) ECHAM5/MPI-OM. (b) ECCO-GODAE.

transport is calculated from zonal wind stress, and the Florida Current transport across the respective boundary current (see Sect. 2 for details). As described above, in the models the mid-ocean transport is taken as the residual = MOC – Florida Current transport – Ekman transport.

The time-mean MOC in ECHAM5/MPI-OM is for the ensemble mean and most ensemble members within the 99% confidence interval of the RAPID/MOCHA MOC estimate (19.1 Sv from RAPID/MOCHA, and 18.7 Sv for the ensemble mean). The time-mean MOC in ECCO-GODAE, 11.4 Sv, is nearly 8 Sv lower than observed (Fig. 7, Table 2). The MOC variability is similar within the 99 percent confidence

interval of the RAPID/MOCHA array for more than half of the ensemble members in ECHAM5/MPI-OM, while MOC variability is lower than observed in ECCO-GODAE (Fig. 7, Table 2).

Both the observed time-mean of 31.7 Sv and the temporal variability of 3.3 Sv of the Florida Current are overestimated in ECHAM5/MPI-OM (by about 10 Sv and about 1 Sv, respectively) and underestimated in ECCO-GODAE (by about 5 Sv and 0.5 Sv, respectively). Note that a strong Florida Current does not necessarily entail a strong MOC and vice versa; a strong Florida Current might merely indicate a strong recirculation. None of the models shows a seasonal variation,

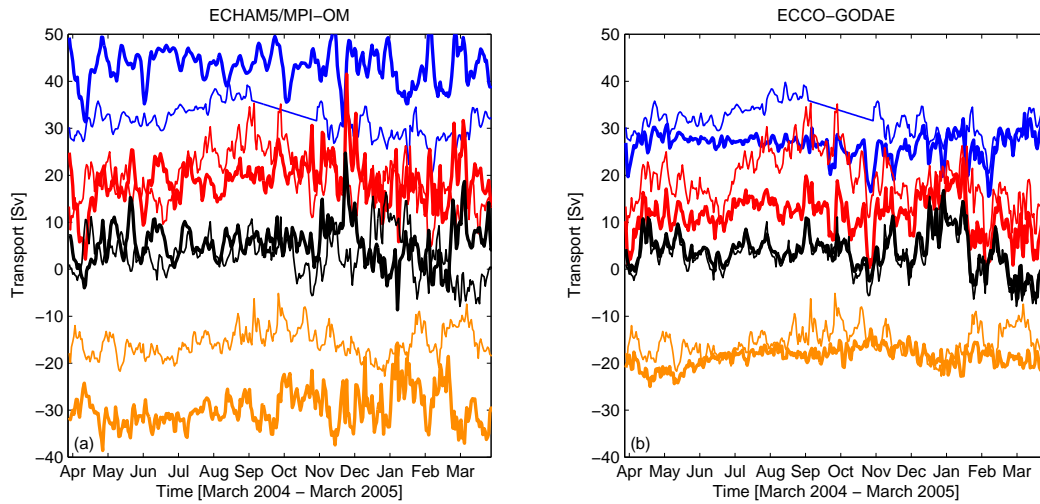


Fig. 7. Integrated transports from RAPID-MOC array (thin; as in Cunningham et al. (2007), Fig. 3) and models (thick): Florida Current (blue), MOC (red), Ekman (black), upper mid-ocean transport (orange). **(a)** ECHAM5/MPI-OM (one realisation). **(b)** ECCO-GODAE.

i.e. increased Florida Current transport in summer. Note that the definition of the Florida Current in ECHAM5/MPI-OM is somewhat subjective (cf. Sect. 2.2), and so are its time-mean and variability. The absence of a topographically confined Straits of Florida in ECHAM5/MPI-OM makes it difficult to distinguish between Gulf Stream variability and Rossby-wave generated variability of the boundary current, and hence the computed Florida Current.

The Ekman transport in ECHAM5/MPI-OM has a larger time-mean than RAPID/MOCHA (about 6 Sv versus about 3 Sv), while the standard deviations are similar to the observed within the 99 percent confidence interval (about 4 Sv). The Ekman transport in ECCO-GODAE has a similar time-mean (3.7 Sv) within the 99% confidence interval of the RAPID/MOCHA estimate, but a slightly smaller variability (3.8 Sv) than RAPID/MOCHA.

The mid-ocean transport is overestimated in ECHAM5/MPI-OM by more than 10 Sv (time-mean), which could again be due to the definition of the Florida Current as we have not tuned the definition to match the time-mean (cf. Sect. 2.2). ECCO-GODAE underestimates the observed variability of 3.1 Sv by 1 Sv in standard deviation.

We summarise the characteristics of the temporal variability of the different transport components in a Taylor diagram (Fig. 8; Taylor, 2001). The standard deviations of the timeseries for the RAPID/MOCHA array are indicated on the abscissa. The smaller the distance of the marker for a certain component in the model is to the respective marker for the RAPID/MOCHA estimate, the closer their agreement. The correlation between two timeseries can be read off at the outer circle. Timeseries with similar magnitude of temporal

Table 3. Different definitions of the mid-ocean transport in the numerical models: time-mean, and standard deviations (std) (all in [Sv]).

	ECHAM5/MPI-OM		ECCO-GODAE	
	mean	std	mean	std
(I) Simulated RAPID/MOCHA array	-39.1	4.8	-17.7	1.4
(II) Residual	-29.7	3.8	-18.8	2.1

variability lie on the same circle around the zero point. Note that this diagram includes no statement about the time-mean transport.

Figure 8 indicates generally higher correlations between ECCO-GODAE and RAPID/MOCHA than between ECHAM5/MPI-OM and RAPID/MOCHA. For ECCO-GODAE, both the Ekman transport correlation of 0.9, and the MOC correlation of 0.6 are within the 95% confidence interval of the RAPID/MOCHA timeseries, using an integral timescale of 24 days, and in turn 15 degrees of freedom (Cunningham et al., 2007). The Ekman transport in ECCO-GODAE and RAPID/MOCHA relies partly on the same source, since ECCO-GODAE uses both NCEP and QuickScat forcing, and the Ekman transport in RAPID/MOCHA was calculated from the QuickScat data. ECCO-GODAE does not exhibit the observed stronger Florida Current transport in summer, which limits the correlation considerably. The level of variability in the ECCO-GODAE solution, however, is generally smaller than in the RAPID/MOCHA estimate.

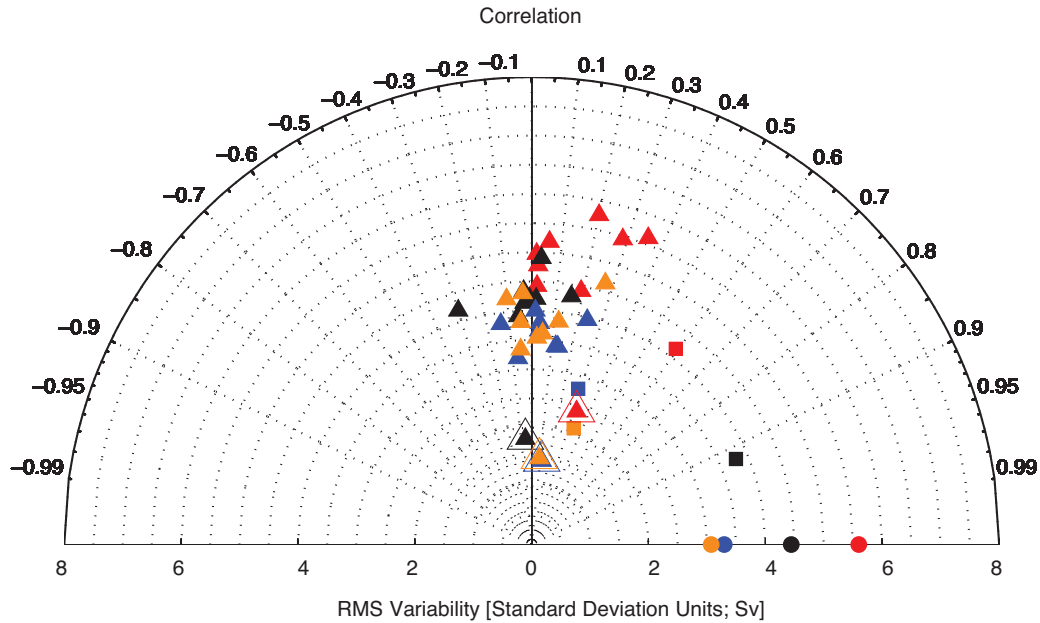


Fig. 8. Taylor diagram for RAPID array observations (circles), ECHAM5/MPI-OM (triangles; framed triangles represent the ensemble mean) and ECCO-GODAE (squares): Florida Current (blue), MOC (red), Ekman (black), mid-ocean transport (orange).

Correlations between the RAPID/MOCHA estimate and ECHAM5/MPI-OM rarely exceed 0.3; the ensemble members exhibit very similar characteristics. This result is not surprising, since neither the ocean nor the atmosphere component are constrained to observations. Hence the timing of anomaly events is likely to be random, and only the analysis of the degree of temporal variability in ECHAM5/MPI-OM is meaningful. Given the substantial differences between RAPID/MOCHA and ECHAM5/MPI-OM in the hydrographic characteristics and the layer transports, it is somewhat surprising that the ECHAM5/MPI-OM MOC and its transport components have a level of variability that is close to the RAPID/MOCHA array. The eight ensemble members all center around the observed level of temporal variability for the respective transport. The ensemble mean generally does not represent an improvement over a single ensemble member for either the level of variability or for the correlation (Fig. 8).

4 Discussion

The results from the first year of the RAPID/MOCHA array at 26.5° N in the Atlantic has enabled the first evaluation of a simulated MOC against observational estimates. Simulated short-term MOC variability has rarely been analysed so far, due to the lack of observation-based estimates to assess the models' realism. The present analysis is based on only a one year timeseries as the observations have not yet been published for the subsequent deployment period.

Ultimately, the MOC variability on interannual, decadal and longer timescales has to be understood in both observations and the models.

In ECHAM5/MPI-OM, the MOC, Florida Current transport, and Ekman transport show for half or more of the ensemble members magnitudes of temporal variability similar to RAPID/MOCHA within the 99% confidence interval. Whether the projected variability from long-term climate simulations remains a good estimate of the actual variability, either for a similar or potentially different state of the climate system, is not known. While the close resemblance in the magnitude of simulated MOC variability is reassuring, the large discrepancies in the hydrographic characteristics point to systematic deficiencies whose impacts on long-term climate change projections remain to be established. One source of the discrepancies in the hydrographic characteristics is the model drift, inherent to a model integration spanning several 100 years constrained only by greenhouse gas concentrations, aerosols and orbital forcing. Within the limitations of the currently available observations, the correspondence between the level of variability in RAPID/MOCHA and ECHAM5/MPI-OM increases the confidence in the estimates of the period it takes to detect a change in the MOC based on such a model (e.g. Baehr et al., 2007a, 2008). As the continuous instrumental record, both from the global observing system and from regional monitoring systems such as RAPID/MOCHA, extends in time, these estimated detection times will slowly become verifiable against observations.

ECCO-GODAE shows hydrographic characteristic that are overall similar to the RAPID/MOCHA observations,

except for the lower part of the intermediate waters at the western boundary. Neither the Florida Current cable measurements nor the RAPID/MOCHA observations have so far been used as constraints in the ECCO optimisation. Nevertheless, discrepancies in hydrographic characteristics between RAPID and ECCO-GODAE are smaller than estimated temperature and salinity uncertainties (Forget and Wunsch, 2007). The correspondence between the RAPID/MOCHA array observations and ECCO-GODAE is reassuring. It suggests that a dynamical model that is constrained by the variety of observations available from the global observing system since the early 1990's is able to reproduce the local array measurements. A pure (i.e. free-running) forward integration of the model using ECCO-GODAE's optimised initial state and air-sea fluxes produces hydrographic and transport estimates that agree reasonably well with the RAPID array estimates over the short time span (3 months from January to March 2005) considered. Incorporating the RAPID/MOCHA array and Florida cable measurements into ECCO's estimation framework can be expected to produce a dynamically consistent state estimate, which more closely mimics the MOC derived from the RAPID/MOCHA array, both in its mean and in its temporal structure. Likewise, an incorporation of the RAPID/MOCHA array into ECCO-GODAE should produce an improved representation of the density-driven component of the MOC, i.e. the mid-ocean transport, which is essential for capturing the long-term evolution of the MOC.

Overall, the hydrographic characteristics at 26.5 N simulated in ECCO-GODAE are closer to the RAPID/MOCHA observations than in ECHAM5/MPI-OM, and yet the time-mean of the simulated MOC is closer to the RAPID/MOCHA observations in ECHAM5/MPI-OM than in ECCO-GODAE. In ECHAM5/MPI-OM, there seems to be a fortunate cancellation of deficiencies in the simulation of temperature and salinity. The resulting zonal density gradient is actually stronger than suggested by the observations at intermediate waters, while weaker below 2000 m (cf. Fig. 3). This in turn results in comparatively strong northward and southward transports, i.e. a strong MOC. In ECCO-GODAE, deficiencies mostly occur in the intermediate waters at the western boundary (cf. Fig. 2). Some of these deficiencies are canceled. Although the resulting zonal density gradient has a similar sign than the observations, it is weaker at intermediate waters and stronger below 2000 m than the observations suggest (cf. Fig. 3). This in turn results in comparatively weak northward and southward transports, i.e. a weak MOC.

It has been suggested earlier that on the spatial and temporal scales considered here, random eddy variability plays a sizeable role in MOC variability (cf., Table 2 in the Appendix of ZW01, W07) Over one year, the mid-ocean transport estimated by the RAPID/MOCHA array shows a variability that is smaller by a factor of 4 than the variability approximated by the simple model of Wunsch (2007). In contrast to Wunsch's (2007) assumption of 16 cm root mean

square variability in the sea surface height, observations show a sharp decline towards the western boundary (within 100 km of Abaco Island; Kanzow et al., 2009) resulting in about 3 to 5 cm root mean square variability in the sea surface height. Heuristic theory suggests that boundary waves are responsible for this decline (Kanzow et al., 2009). For the numerical models, the resolution of both models does not permit eddies to be resolved. It is therefore rather surprising how the well the magnitude of variability in all transport components agrees between the RAPID/MOCHA estimate and especially the ECHAM5/MPI-OM coupled model estimate. The underlying question of to what extent should models at 1 or 1.5° horizontal resolution be expected to resolve the full temporal variability presented in the RAPID/MOCHA MOC estimate is beyond the scope of this paper, and therefore left for future study. Combining array-derived transport estimates with a model could help in producing estimates of the representation error of model-derived transports at coarse resolution. Such an error estimate would allow us to assess the reliability of coupled climate models, and their climate change projections, specifically with respect to both long-term MOC changes and the prediction of short-term MOC changes. Moreover, such an error estimate would support the use of oceanic state estimates as initial conditions for climate predictions.

5 Conclusions

We have evaluated the simulated MOC from two numerical models, the global coupled model ECHAM5/MPI-OM and the oceanic state estimation ECCO-GODAE against the MOC timeseries estimated from the RAPID/MOCHA array, and conclude:

- The hydrographic characteristics at 26.5° N are different from the observations in ECHAM5/MPI-OM, but are overall similar to the observations in ECCO-GODAE.
- The observed time-mean of the MOC is very well reproduced in ECHAM5/MPI-OM, but is underestimated in ECCO-GODAE. The observed time-mean values of the MOC transport components are not well reproduced in either model.
- The magnitude of the observed temporal variability of the MOC is very well reproduced in ECHAM5/MPI-OM, but is underestimated in ECCO-GODAE. Both models underestimate the observed mid-ocean transport variability.
- ECHAM5/MPI-OM shows no significant correlations with the observed MOC and its transport components. In contrast, ECCO-GODAE shows significant correlations with the observed MOC and Ekman transport.

Acknowledgements. We wish to thank Gaël Forget and Carl Wunsch for stimulating discussions. Joël Hirschi provided helpful comments on the manuscript. The RAPID/MOCHA mooring operations have been funded by the Natural Environment Research Council, RAPID, and NSF. The Florida Current cable data are made freely available by the Atlantic Oceanographic and Meteorological Laboratory (www.aoml.noaa.gov/phod/floridacurrent/) and are funded by the NOAA Office of Climate Observations. The wind-stress data were obtained from Centre ERS d'Arquive et de Traitement the Institut Français de Recherche pour l'Exploration de la Mer in Plouzané, France. This work was in part supported by the Max Planck Society (HH, JM). The computer simulations for the ECHAM5/MPI-OM model were performed at the DKRZ (Deutsches Klimarechenzentrum) in Hamburg, Germany. ECCO-GODAE is supported by the National Ocean Partnership Program (NOAA, NASA and NSF) with additional funding from NASA.

Edited by: K. J. Heywood

References

- Baehr, J., Haak, H., Alderson, S., Cunningham, S. A., Jungclaus, J., and Marotzke, J.: Timely detection of changes in the meridional overturning circulation at 26°N in the Atlantic, *J. Climate*, 20, 5827–5841, 2007a.
- Baehr, J., Hirschi, J., Beismann, J., and Marotzke, J.: Monitoring the meridional overturning circulation in the North Atlantic: A model-based array design study, *J. Mar. Res.*, 62(3), 283–312, 2004.
- Baehr, J., Keller, K., and Marotzke, J.: Detecting potential changes in the meridional overturning circulation at 26°N in the Atlantic, *Climatic Change*, 91, 11–27, doi:10.1007/s10584-006-9153-z, 2008.
- Baringer, M. O. and Larsen, J. C.: Sixteen years of Florida Current transport at 27°N, *Geophys. Res. Lett.*, 28, 3179–3182, 2001.
- Bryden, H. L., Longworth, H. R., and Cunningham, S. A.: Slowing of the Atlantic meridional overturning circulation at 25°N, *Nature*, 438, 655–657, 2005.
- Cunningham, S. A., Kanzow, T., Rayner, D., Baringer, M. O., Johns, W. E., Marotzke, J., Longworth, H. R., Grant, E. M., Hirschi, J. J.-M., Beal, L. M., Meinen, C. S., and Bryden, H.: Temporal variability of the Atlantic meridional overturning circulation at 26.5°N, *Science*, 317, 935–938, 2007.
- Forget, G. and Wunsch, C.: Estimated global hydrographic variability, *J. Phys. Oceanogr.*, 37, 1997–2008, 2007.
- Giering, R. and Kaminski, T.: Recipes for adjoint code construction, *ACM T. Math. Software*, 24, 437–474, 1998.
- Gouretski, V. and Koltermann, K.: WOCE global hydrographic climatology. Technical report, Berichte des BSH 35/2004, Bundesamt fuer Seeschifffahrt und Hydrographie, Hamburg und Rostock, Germany, 2004.
- Graf, J., Sasaki, C., Winn, C., Liu, W. T., Tsai, W., Freilich, M., and Long, D.: NASA Scatterometer Experiment, *Acta Astronaut.*, 43(7–8), 397–407, 1998.
- Hall, M. M. and Bryden, H. L.: Direct estimates and mechanisms of ocean heat transport, *Deep-Sea Res.*, 29(3A), 339–359, 1982.
- Heimbach, P., Hill, C., and Giering, R.: An efficient exact adjoint of the parallel MIT general circulation model, generated via automatic differentiation, *Future Gener. Comp. Sy.*, 21(8), 1356–1371, doi:10.1016/j.future.2004.11.010, 2005.
- Hirschi, J., Baehr, J., Marotzke, J., Stark, J., Cunningham, S., and Beismann, J.-O.: A monitoring design for the Atlantic meridional overturning circulation, *Geophys. Res. Lett.*, 30(7), 1413, doi:10.1029/2002GL016776, 2003.
- Johns, W. E., Beal, L. M., Baringer, M. O., Molina, J., Cunningham, S. A., Kanzow, T., and Rayner, D.: Variability of shallow and deep western boundary currents off the Bahamas during 2004–2005: First results from the 26N RAPID-MOC array, *J. Phys. Oceanogr.*, 38, 605–623, 2007.
- Jungclaus, J. H., Botzet, M., Haak, H., Luo, J., Latif, M., Marotzke, J., Mikolajewicz, U., and Roeckner, E.: Ocean circulation and tropical variability in the coupled model ECHAM5/MPI-OM. *J. Climate*, 19, 3952–3972, 2006.
- Kanzow, T., Johnson, H., Marshall, D., Cunningham, S. A., Hirschi, J. J.-M., Mujahid, A., Bryden, H. L., and Johns, W. E.: Basin-wide integrated volume transports in an eddy-filled ocean. *J. Phys. Oceanogr.*, accepted, 2009.
- Kanzow, T., Cunningham, S. A., Rayner, D., Hirschi, J. J.-M., Johns, W. E., Baringer, M. O., Bryden, H. L., Beal, L. M., Meinen, C. S., and Marotzke, J.: Observed flow compensation associated with the MOC at 26.5°N in the Atlantic, *Science*, 317, 938–941, 2007.
- Köhl, A. and Stammer, D.: Variability of the meridional overturning in the North Atlantic from 50 years GECCO state estimation, *J. Phys. Oceanogr.*, 38, 1913–1930, 2008.
- Köhl, A., Stammer, D., and Cornuelle, B.: Interannual to decadal changes in the ECCO global synthesis, *J. Phys. Oceanogr.*, 37, 313–337, 2007.
- Larsen, J. C.: Florida current volume transports from voltage measurements, *Science*, 277, 302–304, 1985.
- Longworth, H. R. and Bryden, H. L.: Ocean circulation: mechanisms and impacts – past and future changes of meridional overturning., volume: AGU Geophysical Monograph 173, chapter: Discovery and quantification of the Atlantic Meridional Overturning Circulation: the importance of 25N, Washington DC, USA, American Geophysical Union, 5–18, 2007.
- Marotzke, J., Cunningham, S. A., and Bryden, H. L.: Monitoring the Atlantic meridional overturning circulation at 26.5°N, Proposal accepted by the Natural Environment Research Council (UK), online available at: <http://www.noc.soton.ac.uk/rapidmoc/>, last access: 15 November 2009, 2002.
- Marotzke, J., Giering, R., Zhang, K. Q., Stammer, D., Hill, C., and Lee, T.: Construction of the adjoint MIT ocean general circulation model and application to Atlantic heat transport sensitivity, *J. Geophys. Res.*, 104, 29529–29547, 1999.
- Marshall, J., Hill, C., Perelman, L., and Adcroft, A.: Hydrostatic, quasi-hydrostatic and nonhydrostatic ocean modeling, *J. Geophys. Res.*, 102(C3), 5733–5752, 1997.
- Marsland, S. J., Haak, H., Jungclaus, J. H., Latif, M., and Röske, F.: The Max-Planck-Institute global ocean/sea ice model with orthogonal curvilinear coordinates, *Ocean Model.*, 5, 91–127, 2003.
- Meinen, C. S., Garzoli, S. L., Johns, W. E., and Baringer, M. O.: Transport variability of the Deep Western Boundary Current and the Antilles Current off Abaco Island, Bahamas, *Deep-Sea Res. I*, 11(51), 1397–1415, 2004.
- Nakicenovic, N. and Swart, R.: Special report on emission

- scenarios, Technical report, Intergovernmental Panel on Climate Change (IPCC), 2000.
- Rayner, D.: RRS Discovery Cruise D277/D278 RAPID mooring cruise report February–March 2004, Technical report, Southampton Oceanography Centre, Southampton, 2005.
- Roeckner, E., Bäuml, G., Bonaventura, L., Brokopf, R., Esch, M., Giorgetta, M., Hagemann, S., Kirchner, I., Kornbluh, L., Manzini, E., Rhodin, A., Schlese, U., Schulzweida, U., and Tompkins, A.: The atmospheric general circulation model ECHAM5, part I: Model description, Max Planck Institute for Meteorology, Technical Report 349, 2003.
- Roemmich, D. and Wunsch, C.: Two transatlantic sections: Meridional circulation and heat flux in the subtropical North Atlantic Ocean, *Deep-Sea Res.*, 32(6), 619–664, 1985.
- Stammer, D., Wunsch, C., Giering, R., Eckert, C., Heimbach, P., Marotzke, J., Adcroft, A., Hill, C. N., and Marshall, J.: Global circulation during 1992–1997, estimated from ocean observations and a general circulation model, *J. Geophys. Res.*, 107(C9), 3118–3155, 2002.
- Stammer, D., Wunsch, C., Giering, R., Eckert, C., Heimbach, P., Marotzke, J., Adcroft, A., Hill, C. N., and Marshall, J.: Volume, heat and freshwater transports of the global ocean circulation 1993–2000, estimated from a general circulation model constrained by World Ocean Circulation Experiment (WOCE) data, *J. Geophys. Res.*, 108(C1), 3007–3030, 2003.
- Taylor, K. E.: Summarizing multiple aspects of model performance in a single diagram, *J. Geophys. Res.*, 106(D7), 7183–7192, 2001.
- Wunsch, C.: On measuring mass transport variability in an eddy-filled ocean, *Nat. Geosci.*, 1, 165–168, 2007.
- Wunsch, C. and Heimbach, P.: Estimated decadal changes in the North Atlantic meridional overturning circulation and heat flux 1993–2004, *J. Phys. Oceanogr.*, 36, 2012–2024, 2006.
- Wunsch, C. and Heimbach, P.: Practical global oceanic state estimation, *Physica D*, 230, 197–208, 2007.
- Zang, X. and Wunsch, C.: Spectral description of low-frequency oceanic variability, *J. Phys. Oceanogr.*, 31, 3073–3095, 2001.